Published in final edited form as:
Anesthesiology. 2014 June ; 120(6): 1463–1475. doi:10.1097/ALN.0000000000000176.

Enhanced Excitability of Primary Sensory Neurons and Altered Gene Expression of Neuronal Ion Channels in Dorsal Root Ganglion in Paclitaxel-Induced Peripheral Neuropathy

Haijun Zhang, M.D.[*] and **Patrick M. Dougherty, Ph.D.**
Department of Pain Medicine, The University of Texas MD Anderson Cancer Center, Houston, TX 77030

Abstract

Background—The mechanism of chemotherapy-induced peripheral neuropathy after paclitaxel treatment is not well understood. Given the poor penetration of paclitaxel into central nervous system, peripheral nervous system is most at risk.

Methods—Intrinsic membrane properties of dorsal root ganglion (DRG) neurons were studied by intracellular recordings. Multiple-gene real-time Polymerase Chain Reaction array was used to investigate gene expression of DRG neuronal ion channels.

Results—Paclitaxel increased the incidence of spontaneous activity from 4.8% to 27.1% in large and from 0% to 33.3% in medium-sized neurons. Paclitaxel decreased the rheobase (nA) from 1.6 ± 0.1 to 0.8 ± 0.1 in large, from 1.5 ± 0.2 to 0.6 ± 0.1 in medium-sized, and from 1.6 ± 0.2 to 1.0 ± 0.1 in small neurons. After paclitaxel, other characteristics of membrane properties in each group remained the same except that Aδ neurons showed shorter action potential fall time (ms) (1.0 ± 0.2, n = 10 vs. 1.8 ± 0.3, n = 9, paclitaxel vs. vehicle). Meanwhile, real-time polymerase chain reaction array revealed an alteration in expression of some neuronal ion channel genes including upregulation of HCN1 (fold change 1.76 ± 0.06) and $Na_v1.7$ (1.26 ± 0.02) and downregulation of K_{ir} channels ($K_{ir}1.1$, 0.73 ± 0.05, $K_{ir}3.4$, 0.66 ± 0.06) in paclitaxel-treated animals.

Conclusions—The increased neuronal excitability and the changes in gene expression of some neuronal ion channels in DRG may provide insight into the molecular and cellular basis of paclitaxel neuropathy, which may lead to novel therapeutic strategies.

Introduction

Chemotherapy-induced peripheral neuropathy (CIPN) is a very common side effect of paclitaxel (Taxol®, Bristol-Myers Squibb, New York, NY), a widely used chemotherapeutic agent, which severely limits its anticancer application[1]. Although the mechanisms are not well understood, the symptoms of paclitaxel CIPN include prominent numbness, tingling, and occasionally shooting/burning pain[2–4], suggesting a polyneuropathy affecting both

Corresponding author: Haijun Zhang, M.D., Department of Pain Medicine, The University of Texas MD Anderson Cancer Center, 1515 Holcombe Blvd, Y6.5710, U110, Houston, TX 77030, Tel: 713-745-3045, Fax: 713-794-4590 haijun.hj@gmail.com.
[*]Current address: Department of Anesthesiology, The University of Texas Medical School at Houston, Houston, TX 77030

The authors declare no competing interests.

myelinated (Aβ and Aδ) and, less frequently, unmyelinated (C) fibers[2]. Only a very low level of paclitaxel was detected in spinal cord and other parts of central nervous system after repeated administration, but a high concentration of paclitaxel was found in dorsal root ganglia (DRG)[5], possibly due to the dense vascularization in DRG by highly permeable capillaries[6]. The accumulation of paclitaxel in the peripheral nervous system imposes a greater risk for damage to these tissues.

Primary sensory neurons in DRG receive signals generated from peripheral nerve endings, integrate and transfer these signals to spinal cord. Because DRG neurons play a critical role in transducing sensory signals including pain, numerous studies have focused on its involvement in the development of acute and chronic pain in various pathological conditions (for review, see[7]). Extensive studies have revealed that the intrinsic membrane properties of DRG neuronal soma, including both myelinated and unmyelinated cells, are significantly altered following peripheral nerve injury or inflammation, and play important roles in the development of spontaneous pain, hyperalgesia and allodynia. For example, an increased incidence of ectopic discharges originating from the soma of different populations of DRG neurons are commonly found after peripheral nerve injury[8–11], direct compression of the ganglion[12–20] and inflammation[21;22]. A substantial number of DRG neurons showed decreased rheobase and increased responses to either electrical or chemical stimulation applied to the soma[14;15;17;18;20;22–24]. More importantly, blocking such enhanced activities of DRG neurons attenuate chronic pain behavior including spontaneous pain and tactile allodynia[22;25–30].

It is not known whether the intrinsic membrane properties of primary sensory neurons in DRG are altered following exposure to paclitaxel chemotherapy. This gap in knowledge was addressed in the present study using *in vitro* intracellular recordings from the somata of both myelinated and unmyelinated neurons in an intact DRG preparation using rats that had received paclitaxel or vehicle treatment. In addition, multiple-gene real-time polymerase chain reaction (rtPCR) array for neuronal ion channels was conducted to examine the changes in gene expression of neuronal ion channels in DRG from animals with paclitaxel CIPN.

Materials and Methods

Animals

Adult male Sprague-Dawley rats (8–12 weeks, Harlan, Houston, TX) housed in a 12 h light/dark cycle with free access to food and water were used in all experiments. The studies were approved by the Institutional Animal Care and Use Committee at The University of Texas M. D. Anderson Cancer Center and were performed in accordance with the National Institutes of Health Guidelines for Use and Care of Laboratory Animals.

Paclitaxel CIPN Model

Animals were treated with paclitaxel as previously described[31–35]. Paclitaxel (TEVA Pharmaceuticals, Inc. North Wales, PA) solution was given intraperitoneally at a dosage of 2 mg/kg in 0.9% saline every other day for a total of four injections (Day 1, 3, 5, and 7).

Control animals received an equivalent volume of vehicle (cremophor EL/ethanol 1:1). Mechanical hypersensitivity is induced with this treatment protocol by day 7 and lasts at least several weeks (data not shown)[32;33;35;36].

In vitro Intracellular Recording of Intact DRG Neurons

Intracellular recordings were performed after mechanical hypersensitivity has established (usually on days 8 to 14 following chemotherapy)[14]. The L_4 and L_5 ganglia with attached sciatic nerve were removed and then incubated in 1mg/ml Collagenase P (Roche, South San Francisco, CA) and 0.4mg/ml Protease Type XIV (Sigma, St. Louis, MO) for 15 min at 37°C in oxygenated artificial cerebrospinal fluid (ACSF). ACSF contains (mM): 130 NaCl, 24 $NaHCO_3$, 3.5 KCl, 1.25 NaH_2PO4, 1.2 $MgCl_2$, 1.2 $CaCl_2$ and 10 Dextrose (PH = 7.3). After incubation, the ganglia were transferred to a recording chamber and superfused continuously with ACSF bubbled with 95% O_2 + 5% CO_2 at 37°C. The peripheral nerve was stimulated by a suction electrode. All chemicals were purchased from Sigma except where noted.

Intracellular recordings were obtained under current clamp (MultiClamp 700A, Axon Instruments, Sunnyvale, CA) by a glass sharp electrode (Sutter Instruments, Novato, CA) with impedances of 60 – 80 MΩ when filled with 3M KCl. Electrophysiological signals were filtered at 5 kHz, digitized at 20 kHz via a Digidata 1320A interface, and analyzed offline with pClamp 10.0 software (Axon Instruments). All neuron accepted have resting membrane potentials more negative than −45 mV. Baseline activity was first monitored for 2 minutes without the delivery of any external stimuli to detect spontaneous activity (SA). Cells showing high levels of SA that would confound interpretation of responses to external stimuli were not further characterized. If there was either no or only low levels of SA, a series of electric stimuli (1–5 mA, duration 0.05 ms for A-fiber and 0.5 ms for C-fiber) was delivered to the nerve through the suction electrode to induce action potentials (APs) from the soma. The axonal conduction velocity (CV) was calculated by dividing the latency of the evoked AP into the distance between the stimulating electrode and the center of the ganglion (usually 12 – 15 mm). After the completion of peripheral nerve stimulation, the recorded cell was depolarized by a series of 40-ms injecting currents from −0.05 nA to 3 nA in increments of 0.025 nA to induce one or more APs. The current threshold (rheobase) was defined as the minimal current that evoked an AP through intracellular sharp electrode. The input resistance of each cell was measured based on the steady-state voltage changes at the end of the application of a series of hyperpolarizing/depolarizing currents (−50 pA to 50 pA, ΔI = 25 pA, duration 40 ms). Repetitive discharges of each neuron were measured by counting the spikes evoked by injecting a 1-s depolarizing current at 2 times the threshold.

Neurons with CV were divided into three groups as previously reported[14;15;37;38]: C-neurons < 1.3 m/s, Aδ-neurons 1.3 – 12 m/s, and Aα/β-neurons > 12 m/s. Additional characteristics of the AP including amplitude, duration, rise time and fall time, amplitude and 50% duration (measured at an amplitude half way between) of afterhyperpolarization were measured.

Multiple-Gene real-time Polymerase Chain Reaction Neuronal Ion Channels Array

DRG tissues used for rtPCR array were collected on Day 7 after paclitaxel or vehicle treatment (twelve rats were treated with paclitaxel and four rats were treated with vehicle) as previously described[35]. Animals were perfused transcardially with cold phosphate-buffered saline before tissue collection. L4 and L5 DRGs from both sides were collected (four ganglia per rat). DRG tissues from animals with the same treatment were pooled together (four rats per group) during tissue processing. Total RNA was extracted using TRIzol reagent (Invitrogen, Carlsbad, CA) and further purified using the RNeasey Mini Kit (Qiagen, Valencia, CA). The concentration and purity of RNA were detected by measuring the absorbance at 260 and 280 nm using a spectrophotometer (NanoDrop 2000, Thermo Scientific, Odessa, TX). Reverse transcription of complementary DNA (cDNA) from 2 μg of total RNA was performed in a thermal cycler (GeneAmp Polymerase Chain Reaction System 9700, Life Technologies, Carlsbad, CA) by RT^2 First Strand Kit (Qiagen) according to manufacturer's instruction (RT^2 Profiler PCR Array Handbook, Qiagen). The proprietary procedure effectively eliminated possible contaminating genomic DNA from RNA samples before reverse transcription. The amplification of cDNA was performed using RT^2 SYBR Green ROX qPCR Mastermix (Cat. no. 330521, Qiagen). The neuronal ion channels array was performed using rat 384-well RT^2 Profiler PCR Array Kit (Cat. no. 330231, PARN-036ZA, Qiagen) on a 7900 Sequence Detection system (Life Technologies). Amplification steps consisted of one cycle of 50°C for 2 minutes plus 95°C for 10 minutes, 40 cycles of 95°C for 15 seconds, 60°C for 1 minute, and one cycle of 95°C for 15 seconds, 60°C for 15 seconds and 95°C for 15 seconds as a dissociation stage. The gene expression data was uploaded and analyzed using the online PCR array data analysis tool* (version 3.0, Qiagen). The threshold cycle (*Ct*; the number of cycles to reach the threshold of detection) was determined for each gene and the relative expression level of each gene was calculated using the following formula[39]: relative expression of messenger RNA = $2^{-\Delta[(Ct\ \text{sample} - Ct\ \text{control})_{\text{paclitaxel}} - (Ct\ \text{sample} - Ct\ \text{control})_{\text{vehicle}}]}$, where Ct_{sample} is the *Ct* for the target gene and Ct_{control} is the average *Ct* for several housekeeping genes including β-actin, β-2 microglobulin, hypoxanthine phosphoribosyltransferase 1, lactate dehydrogenase A, and ribosomal protein P1. Positive and negative control wells were used to access reverse transcription efficiency, presence of genomic DNA and positive rtPCR reactions according to manufacturer's instruction. To minimize the variance caused by sample handling and processing, all samples were processed by the same experimenter with the same experiment protocol, all cDNA were synthesized and amplified on the same plate at the same time.

Statistical Analysis

All results are presented as means ± SEM (which only reaches a 68% confidence interval) and analyzed with Prism GraphPad 6.0 (GraphPad Software, Inc., La Jolla, CA) or Sigma Plot 11.0 (Systat Software, Inc., San Jose, CA). For electrophysiological results, differences between means were tested for significance using One-way ANOVA with Turkey's multiple comparison or Mann Whitney *U*-test (comparison was made across all six groups within the same family). The difference in incidence was analyzed with chi-square test. For rtPCR

*http://pcrdataanalysis.sabiosciences.com/pcr/arrayanalysis.php. Last date accessed Aug 20th, 2013.

results, the difference between paclitaxel and vehicle treatment was expressed by fold changes (comparing to vehicle group) and analyzed using one-sample *t*-test with the hypothesis that the actual fold change of each ion channel after paclitaxel was not different from the hypothesized value 1.0. The Bonferroni correction was later applied in the multiple testing. The difference is considered as statistically significant with an alpha value of $P < 0.05$ and the term "significant" means statistically significant unless otherwise noted. The investigators were not blinded with the groups.

Results

One hundred and eighty DRG neurons, including 111 from paclitaxel-treated rats (23 rats) and 69 from vehicle-treated rats (11 rats), recorded with sharp electrode were included for further analysis. The neurons were first grouped according to their size as small (<= 30 um), medium-sized (31 – 44 um), and large (>= 45 um) cells. It has been shown by different studies that the classification of DRG neurons by the diameter of the soma yielded virtually the same groups of neurons as a classification by their axonal conduction velocity[14;18;40]. Seventy large, 21 medium-sized and 20 small neurons were from paclitaxel-treated animals. Forty two large, 14 medium-sized and 13 small neurons were from vehicle-treated animals.

Increased Excitability of DRG Neurons after Paclitaxel Chemotherapy

Spontaneous Activity—SA was observed in 26 neurons from paclitaxel-treated animals (26/111, 23.4%) but in only 2 neurons from vehicle-treated animals (2/69, 2.9%). SA was recorded in 19 of 70 (27.1%) large neurons and in 7 of 21 (33.3%) medium-sized neurons in paclitaxel-treated animals. Two of 42 (4.8%) large neurons from vehicle-treated animals showed SA. No SA was observed in small neurons from either group. The incidence of SA was significantly increased after paclitaxel treatment (Fig. 1 A).

The patterns of SA were classified as irregular, regular-continuous, and bursting as previously described[8;15;17]. Of the 28 spontaneously discharging neurons (26 from paclitaxel- and 2 from vehicle-treated groups), 15 cells displayed irregular discharges, including 10 large and 5 medium-sized neurons from paclitaxel-treated animals. Consistent with the previous reports on the study of peripheral nerve injury[8] and compressed ganglion[15;17], irregular SA was the most common pattern observed (53.6%) in paclitaxel CIPN. In this category, one cell displayed a mixture of doublet and single spikes (data not shown) while all others showed irregular inter-spike intervals (Fig. 1B). Nine cells, including 6 large and 1 medium-sized neurons from paclitaxel- and 2 large neurons from vehicle-treated animals, showed regular and continuous discharges which was the second most common discharge pattern in the study (32.1%) (Fig. 1C). Bursting discharge, the least common discharge pattern (14.3%), was observed in 4 cells including 3 large and 1 medium-sized neurons from paclitaxel-treated animals (Fig. 1D).

Resting Membrane Potential—Both large and medium-sized neurons with SA were depolarized compared to the quiescent cells (neurons that did not show SA) in the same size group in paclitaxel-treated animals (−51.6 ± 1.7, n = 19 vs. −57.3 ± 0.9, n = 51, p = 0.009 for large cells; −46.3 ± 0.9, n = 7 vs. −57.4 ± 1.6, n = 14, p = 0.003 for medium-sized cells, one-way ANOVA). For quiescent cells, AP was first induced by intracellular current

injection to verify the ability of the recorded neuron to fire (Fig. 2A). There were no statistically significant differences observed in resting membrane potential for large, medium-sized or small neurons after paclitaxel treatment (Fig. 2B, Table 1).

Increased Excitability of DRG Neurons After Paclitaxel Chemotherapy—The excitability of each quiescent cell was measured by current threshold (Fig. 2A). The current threshold in each category, including large ($P < 0.0001$, one-way ANOVA) and medium-sized ($P < 0.001$) neurons, was significantly lower in paclitaxel-treated animals than that in vehicle-treated animals (Fig. 2C, Table 1). No difference was observed in small cells ($P = 0.067$). DRG neurons often showed increased number of APs evoked by either peripheral nerve stimulation[15] or a long depolarizing current injected intracellularly[14;23] after injury or inflammation. In the present study, the number of APs evoked by a 1-s current injection of 2X current threshold through intracellular electrode was compared. Only cells that showed more than one AP to the stimulation were included in the analysis. Although there was no statistically significant difference in the number of evoked AP for any of the groups after paclitaxel treatment, medium-sized neurons tended to have more APs in response to the depolarizing current in paclitaxel-treated group (Fig. 2D, Table 1). This lack of difference is possibly due to the small number of samples collected. No significant difference was found in input resistance for any of the groups after paclitaxel treatment (Fig. 2E).

Characteristics of DRG Neuron Action Potentials Evoked by Peripheral Nerve Stimulation—An AP was evoked by delivering electric stimulation through peripheral nerve in 55 (including 7 SA cells) of 111 cells (49.5%) from paclitaxel-treated animals and in 35 (including 1 SA cell) of 69 cells (50.7%) from vehicle-treated animals (Fig. 3A). The proportion of neurons showing nerve stimulation-evoked AP was similar in paclitaxel- and vehicle-treated groups, which was consistent with the report that roughly half of the L4/L5 DRG neurons have axons in the sciatic nerve in rats[41]. CV (Fig. 3B) and some characteristics of evoked AP including amplitude (Fig. 3C), duration (Fig. 3D), rise time (Fig. 3E), fall time (Fig. 3F), afterhyperpolarization amplitude (Fig. 3G) and 50% duration (Fig. 3H) were measured from these neurons and listed in Table 2. No significant difference was observed in CV or any of the characteristics of evoked AP between paclitaxel- and vehicle-treated groups for each size category, except that Aδ neurons showed shorter AP fall time after paclitaxel treatment (Fig. 3F, $p = 0.035$, one-way ANOVA).

Changes in Gene Expression of Multiple Neuronal Ion Channels in DRG after Paclitaxel Chemotherapy

Many molecular and cellular factors, including expression and function of neuronal ion channels, may contribute to the excitability of DRG neurons in chronic pain condition[7]. Changes in gene expression of neuronal ion channels in DRG (L4/L5) from animals with verified mechanical hypersensitivity after paclitaxel chemotherapy was detected using multiple-gene rtPCR array. The array detects 84 different neuronal ion channel genes including 43 potassium, 12 calcium, 9 sodium, 12 transient receptor potential (TRP), 3 chloride and 3 neuronal amiloride-sensitive cation channels, 1 potassium-chloride transporter and bestrophin 1 (see Appendix 1 for the complete list). Using one-sample t-test with Bonferroni correction ($p = 0.05/84 = 0.0006$), none of the changes reached statistical

significance. When Bonferroni correction was not performed, ten genes were found to have significant changes after paclitaxel treatment, including 7 potassium, 1 calcium, 1 sodium, 1 transient receptor potential channels. Seven genes were upregulated including $K_v1.2$, $K_v11.3$, $K_{ir}3.1$, HCN1, TRPV3, $Na_v1.7$ and brain ryanodine receptor-calcium release channel, and three genes were downregulated including $K_{ir}1.1$, $K_{ir}3.4$, and $K_{2P}1.1$ (Table 3). We also highlighted the genes with fold change > 1.2 or < 0.8 compared to vehicle-treated animals and the C*t* value < 33 (which is more conservative than the default cutoff value 35 by manufacturer's handbook) in both paclitaxel and vehicle groups since these genes were considered to have marginal changes and may have potential biological impacts in paclitaxel CIPN. By this criterion, another twenty one genes were modified by paclitaxel treatment (Table 3).

Discussion

Paclitaxel Chemotherapy Increases the Excitability of DRG Neurons

Recordings from peripheral nerve fibers have found that paclitaxel treatment induces increased SA of both myelinated (A-) and unmyelinated (C-) fibers[42] and enhanced responses of C-fibers to peripheral mechanical stimulation[34] using similar paclitaxel CIPN animal models. Since both studies used teased fiber recordings of peripheral nerve (sural and saphenous nerves) with transected central end but intact skin innervation, the recorded axonal activities originated from periphery. The data shown here provided evidence that increased excitability of soma of DRG neurons is induced as well in paclitaxel CIPN and hyperexcitability measured by the intrinsic membrane properties is observed in both myelinated (Aβ and Aδ) and unmyelinated (C) cells.

Around one third of myelinated neurons displayed SA when recorded from the soma after paclitaxel chemotherapy, which is higher than the incidence of SA recorded from peripheral A-fibers[42]. Since patients with paclitaxel CIPN often complain about spontaneous numbness and tingling which indicate myelinated fiber neuropathy[2–4], the prominent hyperexcitability of Aβ and Aδ neurons in DRG may well account for those major sensory dysfunctions in patients with paclitaxel CIPN, as well as tactile allodynia which is consistently observed in paclitaxel CIPN animal models. The increased incidence of SA (ectopic discharges or ectopia) originated from the soma of DRG neurons, especially myelinated cells, has been found across various models of peripheral nerve injury[8–20]. Because the degree of allodynia correlates with the degree of ectopia[8;25;43;44] and blocking the increased activities of DRG neurons attenuate chronic pain behavior including spontaneous pain and allodynia[22;25–30], it has been thought that the hyperexcitability of DRG neurons, particularly myelinated cells, plays a critical role in the initiation of spontaneous pain and tactile allodynia[45]. In addition with the increased incidence of SA, we also found a robust decrease in the rheobase of DRG non-SA neurons, which is similar to the observation after peripheral nerve injury[11;14;15;17;18;20;23;24;46].

The rheobase of DRG small neurons also decreased after paclitaxel treatment, but such a decrease did not reach statistically significant. Although we did not observe SA from soma of nociceptive neurons in our study, the possibility of such activity could not be excluded. Due to the large heterogeneity of DRG neurons, it is possible that the important effects of

paclitaxel may be restricted to particular subclasses of small neurons which were not sampled in the present study. It seems that the incidence of SA originated from the soma of C-cells is quite variable and may depend on different animal models. For example, no or only minimal level of SA in C-cells was observed after spinal nerve axotomy[8;47;48]. A low level of SA from C-cells was found after chronic compression of DRG[13–16;18;19;24;49]. A robust increase in such activity was observed after modified spinal nerve ligation[11;21] or paw inflammation induced by intraplantar Complete Freund's Adjuvant injection[21].

Like previous studies[34;42], we did not find any change in axonal conduction velocity of either myelinated or unmyelinated neurons after paclitaxel chemotherapy. Although it has been reported that paclitaxel induces a reduction of CV in peripheral nerve in experimental animals, these changes seem to depend on the cumulative dosage of paclitaxel since such a reduction only occurred in animals receiving 80 mg/kg but not 16 mg/kg paclitaxel[50] or in mice receiving more than 200 mg/kg[51]. The impact of chemotherapy may also be variable on different types of peripheral nerves because no reduction of CV was found in digital nerve even from mice receiving 200 mg/kg paclitaxel[51]. Finally, the changes in CV may be more prominent closer to the peripheral terminals where die-back occurs since a large increase in CV of muscle afferents after paclitaxel was observed in a recent study[52]. Nevertheless, the lack of change in axonal CV reported here, along with previous studies, may correlate with the observation that low dose of paclitaxel did not induce any axonal degeneration at the mid-axon level[53] but was still sufficient to induce distal terminal degeneration[33;54].

No changes were found in other intrinsic membrane properties including input resistance, AP and AHP amplitude and duration, except that medium-sized neurons had shorter AP fall time in paclitaxel group compared to the same-sized cells in vehicle group. Such a difference could be due to sampling variance since the total duration and rise time of AP in the same group were not changed.

Modulation of Multiple Neuronal Ion Channels May Contribute to Increased Excitability of DRG Neurons after Paclitaxel Chemotherapy

The excitability of DRG neurons is fundamentally determined by the functional activities of neuronal ion channels which could be modulated by many intracellular and extracellular factors in various conditions of chronic pain[7]. In a recent study, multiple-gene rtPCR array has been used to largely confirm the gene changes in both DRG and spinal cord following peripheral nerve injury and inflammation detected by microarray method[55]. This array has also been successfully used to detect robust changes in gene expression of neurotrophin and proinflammatory cytokine in various tissues including DRG after paw plantar incision[56].

With multiple-gene rtPCR array, we have found prominent changes in gene expression of some neuronal ion channels in DRG after paclitaxel chemotherapy. Although the changes in expression of these genes did not reach statistical significance after Bonferroni correction, each did show statistical significance when Bonferroni correction was not performed. Considering the increased probability of false negatives after Bonferroni correction and the high chance of reaching statistical significance when individual rtPCR was performed, we presented these data here.

Although it is impossible to tell which particular channel plays a major role, the robust downregulation of voltage-gated potassium channels such as inwardly rectifying potassium channels (K_{ir} 1.1 and K_{ir} 3.4), and upregulation of hyperpolarization-activated cyclic nucleotide-gated channel 1(HCN1) and voltage-gated sodium channel $Na_v1.7$ suggest the possible involvement of these channels in paclitaxel CIPN. The hyperpolarization-activated current (I_h) medicated by HCN1 is expressed on DRG myelinated neurons[57;58]. The increase of HCN1 may facilitate the increased SA in these neurons observed in the current study. Another striking observation is the increased expression of $Na_v1.7$ in DRG after paclitaxel. $Na_v1.7$ is expressed in both large and small diameter DRG neurons and in most functionally identified nociceptors[59;60]. Studies have shown that gain-of-function mutations of $Na_v1.7$ are strongly linked to some inherited pain disorders such as inherited erythromelalgia[61–63]. Recent studies have established a link between the gain-of-function mutation of $Na_v1.7$ and painful peripheral neuropathy[64;65]. Interestingly, loss-of-function of $Na_v1.7$ has been found being related to insensitivity to pain[66–68]. In addition, animal studies have found that the $Na_v1.7$ expression level in DRG neurons is increased in response to various stimulation and knockdown of $Na_v1.7$ attenuates some pathological pain (for review, see[69]). The specific role of these neuronal ion channels revealed by the current rtPCR study in paclitaxel CIPN remains to be fully established. The ongoing work in the lab is focused on addressing these issues.

There are certainly many limitations to interpret the changes of ion channel gene expression with rtPCR array. For example, the function of these channels depends on multiple factors, such as the rates of protein translation and degradation, post-translational modification and the number of channels expressed on the plasma membrane. Tying the gene expression of these channels to their ultimate function and their specific role in paclitaxel CIPN will need further investigation. Some discrepancies between our study and previous studies have also been noticed. A recent study has shown that TRPV1 mRNA in DRG was increased after paclitaxel and blocking TRVP1 prevented or attenuated mechanical and thermal hypersensitivity of paclitaxel CIPN[70]. A marginal increase in DRG TRPV1 expression was also found in our study, but the difference did not reach statistically significant (see Appendix 1). Another example is that Nav1.2 has been found to be expressed predominantly in brain[71] and only at a very low level in DRG[72;73]. Our data showed that the level of Nav1.2 expression in DRG was comparative with that of Nav1.1, Nav1.9 and Nav1.6 as judged by Ct values (see Appendix 1). These discrepancies could be contributed by several factors such as the variance in the efficiency of RNA extraction or cDNA synthesis between different labs, and the different design of probes.

In conclusion, we show that paclitaxel chemotherapy induces increased excitability of primary sensory neurons in DRG, which is demonstrated by the increased incidence of SA originated from the soma of myelinated cells and decreased rheobase in both myelinated and unmyelinated cells. These alterations in the intrinsic membrane properties of DRG neurons, along with increased activities of peripheral nerve fibers reported by other studies, suggest the pathology of peripheral nervous system may play critical roles in the development of paclitaxel CIPN. The prominent changes in gene expression of some neuronal ion channels in DRG such as upregulation of HCN1 and $Na_v1.7$ channels, and downregulation of K_{ir} channels suggest the possible roles of these channels in paclitaxel CIPN. Our data suggest

the underlying channelopathy mechanism of paclitaxel CIPN and provide potential therapeutic targets.

Supplementary Material

Refer to Web version on PubMed Central for supplementary material.

Acknowledgments

This work was supported by grants from National Institutes of Health, Bethesda, Maryland, USA (NS 046606) and National Cancer Institute, Bethesda, Maryland, USA (CA12487).

Appendix 1

Gene Expression of Neuronal Ion Channels in DRG after Paclitaxel Chemotherapy

Symbol	Ion Channel Name	Ct				Fold Change (paclitaxel/vehicle)			
		V	P 1	P 2	P 3	P 1	P 2	P 3	Mean
Accn1	amiloride-sensitive cation channel 1, neuronal	24.57	25.08	24.44	24.80	0.803	0.991	0.787	0.860
Accn2	amiloride-sensitive cation channel 2, neuronal	22.73	23.03	21.99	22.35	0.925	1.502	1.202	1.210
Accn3	amiloride-sensitive cation channel 3	21.34	21.74	21.05	21.25	0.865	1.105	0.984	0.985
Best1	bestrophin 1	29.14	28.98	28.86	28.9	1.277	1.101	1.088	1.155
Cacna1a	$Ca_v2.1$	28.39	28.93	27.6	28.2	0.787	1.559	1.052	1.132
Cacna1b	$Ca_v2.2$	26.46	26.86	25.88	26.24	0.865	1.348	1.072	1.095
Cacna1c	$Ca_v1.2$	26.75	27.54	25.95	26.68	0.661	1.569	0.966	1.065
Cacna1d	$Ca_v1.3$	28.61	29.39	27.56	28.26	0.662	1.863	1.172	1.232
Cacna1g	$Ca_v3.1$	31.01	31.98	31.05	30.16	0.582	0.878	1.654	1.038
Cacna1i	$Ca_v3.3$	28.95	29.37	28.05	28.45	0.855	1.677	1.302	1.278
Cacnb1	$Ca_v\beta1$	27.67	28.41	27.31	27.77	0.688	1.163	0.865	0.905
Cacnb2	$Ca_v\beta2$	27.08	27.02	26.65	26.88	1.195	1.217	1.064	1.159
Cacnb3	$Ca_v\beta3$	22.17	23.52	21.79	22.15	0.449	1.181	0.935	0.855
Cacng2	$Ca_v\gamma2$	23.73	23.98	23.64	23.71	0.959	0.960	0.932	0.950
Cacng4	$Ca_v\gamma$ 4	24.89	25.4	24.66	24.6	0.804	1.061	1.127	0.997
Clcn2	Clc2	25.9	27.21	25.64	25.71	0.458	1.079	1.051	0.863
Clcn3	Clc3	22.85	23.15	22.6	22.64	0.929	1.072	1.069	1.023
Clcn7	Clc7	25.53	26.29	24.89	25.24	0.677	1.407	1.131	1.072
Hcn1	HCN1	22.36	22.37	22.46	22.56	1.633	1.842	1.799	1.758
Hcn2	HCN2	23.25	23.78	22.94	23.18	0.795	1.120	0.970	0.962
Kcna1	$K_v1.1$	22.74	23.1	22.32	22.46	0.894	1.210	1.125	1.076
Kcna2	$K_v1.2$	20.96	20.4	20.18	20.29	1.689	1.548	1.462	1.566
Kcna5	$K_v1.5$	26.25	27.5	26.29	26.65	0.482	0.883	0.702	0.689
Kcna6	$K_v1.6$	22.86	23.3	22.37	22.63	0.840	1.263	1.079	1.061

Symbol	Ion Channel Name	Ct				Fold Change (paclitaxel/vehicle)			
		V	P 1	P 2	P 3	P 1	P 2	P 3	Mean
Kcnab1	$K_v\beta1$	22.2	22.34	21.85	21.85	1.043	1.156	1.177	1.125
Kcnab2	$K_v\beta2$	21.71	22	20.99	21.35	0.939	1.494	1.186	1.206
Kcnab3	$K_v\beta3$	29.99	30.69	29.57	29.64	0.707	1.214	1.182	1.034
Kcnb1	$K_v2.1$	23.95	24.73	23.49	23.67	0.664	1.238	1.121	1.008
Kcnb2	$K_v2.2$	22.52	22.84	21.93	22.24	0.920	1.361	1.121	1.134
Kcnc1	$K_v3.1$	24.87	25.27	24.48	24.61	0.870	1.185	1.109	1.055
Kcnc2	$K_v3.2$	27.02	26.97	26.49	26.75	1.182	1.298	1.111	1.197
Kcnd2	$K_v4.2$	28.54	28.35	28.12	27.86	1.303	1.205	1.474	1.327
Kcnd3	$K_v4.3$	23.14	23.8	23.04	23.21	0.726	0.969	0.880	0.858
Kcnh1	$K_v10.1$	24.63	24.8	23.91	24.14	1.013	1.480	1.288	1.260
Kcnh2	$K_v11.1$	27.69	29.22	26.68	27.18	0.397	1.829	1.320	1.182
Kcnh3	$K_v12.2$	35	35	35	35	N/A	N/A	N/A	N/A
Kcnh6	$K_v11.2$	27.88	28.28	27.53	27.49	0.864	1.149	1.204	1.072
Kcnh7	$K_v11.3$	23.07	22.71	22.26	22.56	1.461	1.582	1.314	1.452
Kcnj1	$K_{ir}1.1$	28.88	29.67	29.24	29.04	0.662	0.704	0.823	0.730
Kcnj11	$K_{ir}6.2$	29.01	30	28.55	29.04	0.576	1.238	0.902	0.905
Kcnj12	$K_{ir}2.2$	26.53	27.14	26.39	26.48	0.751	0.992	0.958	0.900
Kcnj13	$K_{ir}1.4$	25.58	25.34	25.26	24.57	1.357	1.127	1.865	1.449
Kcnj14	$K_{ir}2.4$	28.86	31.4	28.28	28.82	0.196	1.346	0.947	0.830
Kcnj15	$K_{ir}4.2$	28.45	28.18	27.72	27.29	1.379	1.497	2.062	1.646
Kcnj16	$K_{ir}5.1$	28.81	29.67	28.77	27.56	0.629	0.928	2.200	1.252
Kcnj2	$K_{ir}2.1$	28.34	28.54	27.99	27.96	0.996	1.148	1.203	1.116
Kcnj3	$K_{ir}3.1$	23.87	23.71	23.24	23.29	1.281	1.404	1.384	1.356
Kcnj4	$K_{ir}2.3$	32	33.48	31.91	31.48	0.410	0.959	1.325	0.898
Kcnj5	$K_{ir}3.4$	27.36	28.42	27.61	27.85	0.548	0.760	0.657	0.655
Kcnj6	$K_{ir}3.2$	26.34	26.37	26.07	26.37	1.117	1.084	0.904	1.035
Kcnj9	$K_{ir}3.3$	27.87	27.74	27.49	27.6	1.251	1.177	1.113	1.180
Kcnk1	$K_{2p}1.1$	22.77	23.56	22.95	22.98	0.660	0.798	0.797	0.752
Kcnma1	$K_{Ca}1.1$	25.44	26.52	24.71	25.37	0.541	1.496	0.966	1.001
Kcnmb4	$K_{Ca}\beta4$	24.42	24.8	24.44	24.49	0.878	0.889	0.875	0.881
Kcnn1	$K_{Ca}2.1$	27.78	28.84	27.25	27.75	0.545	1.297	0.939	0.927
Kcnn2	$K_{Ca}2.2$	24.66	24.39	24.2	24.44	1.382	1.242	1.076	1.233
Kcnn3	$K_{Ca}2.3$	24.98	25.46	24.55	24.72	0.818	1.211	1.106	1.045
Kcnq1	$K_v7.1$	30.18	29.16	28.72	29.75	2.316	2.472	1.243	2.010
Kcnq2	$K_v7.2$	22.83	22.89	22.41	22.71	1.095	1.213	1.002	1.103
Kcnq3	$K_v7.3$	27.95	28.09	27.24	27.54	1.038	1.479	1.227	1.248
Kcns1	$K_v9.1$	25.1	25.85	24.51	24.96	0.682	1.357	1.016	1.018

Symbol	Ion Channel Name	Ct				Fold Change (paclitaxel/vehicle)			
		V	P 1	P 2	P 3	P 1	P 2	P 3	Mean
Ryr3	brain ryanodine receptor-calcium release channel	25.96	25.56	25.06	25.37	1.505	1.692	1.386	1.528
Scn10a	$Na_v1.8$	20.81	21.44	20.48	20.71	0.740	1.130	0.991	0.954
Scn11a	$Na_v1.9$	22.56	23.85	21.97	22.29	0.469	1.362	1.112	0.981
Scn1a	$Na_v1.1$	23.25	23.72	22.24	22.73	0.826	1.824	1.328	1.326
Scn1b	$Na_v\beta1$	22.97	23.71	21.96	22.37	0.683	1.817	1.399	1.299
Scn2a1	$Na_v1.2$	22.39	22.6	21.87	22.21	0.990	1.295	1.047	1.110
Scn2b	$Na_v\beta2$	25.76	26.44	25.09	25.42	0.709	1.435	1.164	1.103
Scn3a	$Na_v1.3$	27.98	28.32	27.47	28.03	0.906	1.292	0.893	1.030
Scn8a	$Na_v1.6$	23.39	23.96	22.65	22.85	0.770	1.506	1.338	1.205
Scn9a	$Na_v1.7$	21.29	21.18	20.77	20.85	1.233	1.291	1.249	1.258
Slc12a5	KCC2	32.48	33.12	31.69	31.7	0.733	1.552	1.575	1.287
Trpa1	TRPA1	22.88	23.3	22.55	22.86	0.853	1.132	0.932	0.972
Trpc1	TRPC1	24.49	24.99	24.07	24.4	0.813	1.210	0.984	1.002
Trpc3	TRPC3	24.06	24.23	24.11	24.23	1.016	0.876	0.824	0.906
Trpc6	TRPC6	26.64	26.96	27.12	26.55	0.914	0.646	0.983	0.848
Trpm1	TRPM1	33.97	35	34.23	34.03	0.559	0.755	0.883	0.733
Trpm2	TRPM2	27.12	27.51	26.31	26.84	0.871	1.589	1.122	1.194
Trpm6	TRPM6	27.05	26.65	26.34	26.72	1.507	1.478	1.161	1.382
Trpm8	TRPM8	23.46	23.67	22.78	23.09	0.989	1.448	1.194	1.210
Trpv1	TRPV1	22.52	22.62	21.95	22.1	1.068	1.341	1.237	1.215
Trpv2	TRPV2	23.72	24.71	23.47	23.65	0.573	1.075	0.968	0.872
Trpv3	TRPV3	27.99	27.39	26.71	26.82	1.727	2.196	2.068	1.997
Trpv4	TRPV4	29.79	30.34	29.75	29.8	0.784	0.928	0.916	0.876

DRG: dorsal root ganglion; Ct: threshold cycle; V: vehicle group; P1: paclitaxel group 1; P2: paclitaxel group 2; P3: paclitaxel group 3.

Reference List

1. Cavaletti G, Marmiroli P. Chemotherapy-induced peripheral neurotoxicity. Nat Rev Neurol. 2010; 6:657–666. [PubMed: 21060341]
2. Dougherty PM, Cata JP, Cordella JV, Burton A, Weng H-R. Taxol-induced sensory disturbance is characterized by preferential impairment of myelinated fiber function in cancer patients. Pain. 2004; 109:132–142. [PubMed: 15082135]
3. Loprinzi CL, Reeves BN, Dakhil SR, Sloan JA, Wolf SL, Burger KN, Kamal A, Le-Lindqwister NA, Soori GS, Jaslowski AJ, Novotny PJ, Lachance DH. Natural history of paclitaxel-associated acute pain syndrome: Prospective cohort study NCCTG N08C1. J Clin Oncol. 2011; 29:1472–1478. [PubMed: 21383290]
4. Reeves BN, Dakhil SR, Sloan JA, Wolf SL, Burger KN, Kamal A, Le-Lindqwister NA, Soori GS, Jaslowski AJ, Kelaghan J, Novotny PJ, Lachance DH, Loprinzi CL. Further data supporting that paclitaxel-associated acute pain syndrome is associated with development of peripheral neuropathy: North Central Cancer Treatment Group trial N08C1. Cancer. 2012; 118:5171–5178. [PubMed: 22415454]

5. Cavaletti G, Cavaletti E, Oggioni N, Sottani C, Minoia C, D'Incalci M, Zucchetti M, Marmiroli P, Tredici G. Distribution of paclitaxel within the nervous system of the rat after repeated intravenous administration. Neurotoxicol. 2000; 21:389–394.
6. Jimenez-Andrade JM, Herrera MB, Ghilardi JR, Vardanyan M, Melemedjian OK, Mantyh PW. Vascularization of the dorsal root ganglia and peripheral nerve of the mouse: Implications for chemical-induced peripheral sensory neuropathies. Mol Pain. 2008; 4:10. [PubMed: 18353190]
7. Gold MS, Gebhart GF. Nociceptor sensitization in pain pathogenesis. Nat Med. 2010; 16:1248–1257. [PubMed: 20948530]
8. Liu C-N, Wall PD, Ben-Dor E, Michaelis M, Amir R, Devor M. Tactile allodynia in the absence of C-fiber activation: Altered firing properties of DRG neurons following spinal nerve injury. Pain. 2000; 85:503–521. [PubMed: 10781925]
9. Liu CN, Devor M, Waxman SG, Kocsis JD. Subthreshold oscillations induced by spinal nerve injury in dissociated muscle and cutaneous afferents of mouse DRG. J Neurophysiol. 2002; 87:2009–2017. [PubMed: 11929919]
10. Wall PD, Devor M. Sensory afferent impulses orginate from dorsal root ganglia as well as from the perphery in normal and nerve injured rats. Pain. 1983; 17:321–339. [PubMed: 6664680]
11. Djouhri L, Fang X, Koutsikou S, Lawson SN. Partial nerve injury induces electrophysiological changes in conducting (uninjured) nociceptive and nonnociceptive DRG neurons: Possible relationships to aspects of peripheral neuropathic pain and parethesias. Pain. 2012; 153:1824–1836. [PubMed: 22721911]
12. Zhang J-M, Donnelly DF, Song X-J, LaMotte RH. Axotomy increases the excitability of dorsal horn ganglion cells with unmyelinated axons. J Neurophysiol. 1997; 78:2790–2794. [PubMed: 9356426]
13. Song XJ, Zhang JM, Hu SJ, LaMotte RH. Somata of nerve-injured sensory neurons exhibit enhanced responses to inflammatory mediators. Pain. 2003; 104:701–709. [PubMed: 12927643]
14. Zhang H, Mei X, Zhang P, Ma C, White FA, Donnelly DF, LaMotte RH. Altered functional properties of satellite glial cells in compressed spinal ganglia. GLIA. 2009; 57:1588–1599. [PubMed: 19330845]
15. Zhang J-M, Song X-J, LaMotte RH. Enhanced excitability of sensory neurons in rats with cutaneous hyperalgesia produced by chronic compression of the dorsal root ganglion. J Neurophysiol. 1999; 82:3359–3366. [PubMed: 10601467]
16. Ma C, LaMotte RH. Multiple sites for generation of ectopic spontaneous activity in neurons of the chronically compressed dorsal root ganglion. J Neurosci. 2007; 27:14059–14068. [PubMed: 18094245]
17. Ma C, Greenquist KW, LaMotte RH. Inflammatory mediators enhance the excitability of chronically compressed dorsal root ganglion neurons. J Neurophysiol. 2006; 95:2098–2107. [PubMed: 16381809]
18. Ma C, LaMotte RH. Enhanced excitability of dissociated primary sensory neurons after chronic compression of the dorsal root ganglion in the rat. Pain. 2005; 113:106–112. [PubMed: 15621370]
19. Song X-J, Hu S-J, Greenquist KW, Zhang J-M, LaMotte RH. Mechanical and thermal hyperalgesia and ectopic neuronal discharge after chronic compression of dorsal root ganglia. J Neurophysiol. 1999; 82:3347–3358. [PubMed: 10601466]
20. Song Y, Li HM, Xie RG, Yue ZF, Song XJ, Hu SJ, Xing JL. Evoked bursting in injured Abeta dorsal root ganglion neurons: A mechanism underlying tactile allodynia. Pain. 2012; 153:657–665. [PubMed: 22237000]
21. Djouhri L, Koutsikou S, Fang X, McMullan S, Lawson SN. Spontaneous pain, both neuropathic and inflammatory, is related to frequency of spontaneous firing in intact C-fiber nociceptors. J Neurosci. 2006; 26:1281–1292. [PubMed: 16436616]
22. Weng X, Smith T, Sathish J, Djouhri L. Chronic inflammatory pain is associated with increased excitability and hyperpolarization-activated current (Ih) in C- but not Adelta-nociceptors. Pain. 2012; 153:900–914. [PubMed: 22377439]
23. Zheng JH, Walters ET, Song XJ. Dissociation of dorsal root ganglion neurons induces hyperexcitability that is maintained by increased responsiveness to cAMP and cGMP. J Neurophysiol. 2007; 97:15–25. [PubMed: 17021029]

24. Xie Y, Zhang J, Petersen M, LaMotte RH. Functional changes in dorsal root ganglion cells after chronic nerve constriction in the rat. J Neurophysiol. 1995; 73:1811–1820. [PubMed: 7623082]
25. Sukhotinsky I, Ben-Dor E, Raber P, Devor M. Key role of the dorsal root ganglion in neuropathic tactile hypersensibility. Eur J Pain. 2004; 8:135–143. [PubMed: 14987623]
26. Zhang JM, Li H, Brull SJ. Perfusion of the mechanically compressed lumbar ganglion with lidocaine reduces mechanical hyperalgesia and allodynia in the rat. J Neurophysiol. 2000; 84:798–805. [PubMed: 10938306]
27. Malan TP, Ossipov MH, Gardell LR, Ibrahim M, Bian D, Lai J, Porreca F. Extraterritorial neuropathic pain correlates with multisegmental elevation of spinal dynorphin in nerve-injured rats. Pain. 2000; 86:185–194. [PubMed: 10779675]
28. Lyu YS, Park SK, Chung K, Chung JM. Low dose of tetrodotoxin reduces neuropathic pain behaviors in an animal model. Brain Res. 2000; 871:98–103. [PubMed: 10882788]
29. Blenk KH, Habler HJ, Janig W. Neomycin and gadolinium applied to an L5 spinal nerve lesion prevent mechanical allodynia-like behaviour in rats. Pain. 1997; 70:155–165. [PubMed: 9150289]
30. Xie W, Strong JA, Meij JT, Zhang JM, Yu L. Neuropathic pain: Early spontaneous afferent activity is the trigger. Pain. 2005; 116:243–256. [PubMed: 15964687]
31. Polomano RC, Mannes AJ, Clark US, Bennett GJ. A painful peripheral neuropathy in the rat produced by the chemotherapeutic drug, paclitaxel. Pain. 2001; 94:293–304. [PubMed: 11731066]
32. Cata JP, Weng HR, Dougherty PM. The effects of thalidomide and minocycline on taxol-induced hyperalgesia in rats. Brain Res. 2008; 1229:100–110. [PubMed: 18652810]
33. Boyette-Davis J, Xin W, Zhang H, Dougherty PM. Intraepidermal nerve fiber loss corresponds to the development of Taxol-induced hyperalgesia and can be prevented by treatment with minocycline. Pain. 2011; 152:308–313. [PubMed: 21145656]
34. Dina OA, Chen X, Reichling D, Levine JD. Role of protein kinase C[epsi] and protein kinase A in a model of paclitaxel-induced painful peripheral neuropathy in the rat. Neuroscience. 2001; 108:507–515. [PubMed: 11738263]
35. Zhang H, Yoon S-Y, Zhang H, Dougherty PM. Evidence that spinal astrocytes but not microglia contribute to the pathogenesis of paclitaxel-induced painful neuropathy. J Pain. 2012; 13:293–303. [PubMed: 22285612]
36. Cata, JP.; Weng, HR.; Dougherty, PM. 2004 Abstract Viewer/Itinerary Planner. Washington, DC: Society for Neuroscience; 2004. Increased excitability of WDR neurons accompanies paclitaxel - induced hyperalgesia in rats. Program No. 982.4.
37. Waddell PJ, Lawson SN. Electrophysiological properties of subpopulations of rat dorsal root ganglion neurons in vitro. Neuroscience. 1990; 36:811–822. [PubMed: 2234413]
38. Waddell PJ, Lawson SN, McCarthy PW. Conduction velocity changes along the processes of rat primary sensory neurons. Neuroscience. 1989; 30:577–584. [PubMed: 2771039]
39. Schmittgen TD, Livak KJ. Analyzing real-time PCR data by the comparative C(T) method. Nat Protoc. 2008; 3:1101–1108. [PubMed: 18546601]
40. Harper AA, Lawson SN. Conduction velocity is related to morphological cell type in rat dorsal root ganglion neurones. J Physiol. 1985; 359:31–46. [PubMed: 3999040]
41. Devor M, Govrin-Lippmann R. Neurogenesis in adult rat dorsal root ganglia. Neuroscience Letters. 1985; 61:189–194. [PubMed: 4080254]
42. Xiao WH, Bennett GJ. Chemotherapy-evoked neuropathic pain: Abnormal spontaneous discharge in A-fiber and C-fiber primary afferent neurons and its suppression by acetyl-L-carnitine. Pain. 2008; 135:262–270. [PubMed: 17659836]
43. Sheen K, Chung JM. Signs of neuropathic pain depend on signals from injured nerve fibers in a rat model. Brain Res. 1993; 610:62–68. [PubMed: 8518931]
44. Yoon YW, Na HS, Chung JM. Contributions of injured and intact afferents to neuropathic pain is an experimental rat model. Pain. 1996; 64:27–36. [PubMed: 8867245]
45. Devor M. Ectopic discharge in Aβ afferents as a source of neuropathic pain. Exp Brain Res. 2009; 196:115–128. [PubMed: 19242687]
46. Zhu YF, Henry JL. Excitability of Abeta sensory neurons is altered in an animal model of peripheral neuropathy. BMC Neurosci. 2012; 13:15. [PubMed: 22289651]

47. Liu X, Eschenfelder S, Blenk KH, Janig W, Habler H. Spontaneous activity of axotomized afferent neurons after L5 spinal nerve injury in rats. Pain. 2000; 84:309–318. [PubMed: 10666536]
48. Han HC, Lee DH, Chung JM. Characteristics of ectopic discharges in a rat neuropathic pain model. Pain. 2000; 84:253–261. [PubMed: 10666530]
49. Ma C, Shu Y, Zheng Z, Chen Y, Yao H, Greenquist KW, White FA, LaMotte RH. Similar electrophysiological changes in axotomized and neighboring intact dorsal root ganglion neurons. J Neurophysiol. 2003; 89:1588–1602. [PubMed: 12612024]
50. Authier N, Gillet J-P, Fialip J, Eschalier A, Coudore F. Description of a short-term taxol-induced nociceptive neuropathy in rats. Brain Res. 2000; 887:239–249. [PubMed: 11134612]
51. Carozzi VA, Canta A, Oggioni N, Sala B, Chiorazzi A, Meregalli C, Bossi M, Marmiroli P, Cavaletti G. Neurophysiological and neuropathological characterization of new murine models of chemotherapy-induced chronic peripheral neuropathies. Exp Neurol. 2010; 226:301–309. [PubMed: 20832406]
52. Chen X, Green PG, Levine JD. Abnormal muscle afferent function in a model of Taxol chemotherapy-induced painful neuropathy. J Neurophysiol. 2011; 106:274–279. [PubMed: 21562188]
53. Flatters SJ, Bennett GJ. Studies of peripheral sensory nerves in paclitaxel-induced painful peripheral neuropathy: Evidence for mitochondrial dysfunction. Pain. 2006; 122:245–257. [PubMed: 16530964]
54. Flatters SJL, Bennett GJ. Ethosuximide reverses paclitaxel- and vincristine-induced painful peripheral neuropathy. Pain. 2004; 109:150–161. [PubMed: 15082137]
55. Lacroix-Fralish ML, Austin JS, Zheng FY, Levitin DJ, Mogil JS. Patterns of pain: Meta-analysis of microarray studies of pain. Pain. 2011; 152:1888–1898. [PubMed: 21561713]
56. Spofford CM, Brennan TJ. Gene expression in skin, muscle, and dorsal root ganglion after plantar incision in the rat. ANESTHESIOLOGY. 2012; 117:161–172. [PubMed: 22617252]
57. Gao LL, McMullan S, Djouhri L, Acosta C, Harper AA, Lawson SN. Expression and properties of hyperpolarization-activated current in rat dorsal root ganglion neurons with known sensory function. J Physiol. 2012; 590:4691–4705. [PubMed: 22753545]
58. Acosta C, McMullan S, Djouhri L, Gao L, Watkins R, Berry C, Dempsey K, Lawson SN. HCN1 and HCN2 in Rat DRG neurons: levels in nociceptors and non-nociceptors, NT3-dependence and influence of CFA-induced skin inflammation on HCN2 and NT3 expression. PLoS One. 2012; 7:e50442. [PubMed: 23236374]
59. Dib-Hajj SD, Cummins TR, Black JA, Waxman SG. Sodium channels in normal and pathological pain. Annu Rev Neurosci. 2010; 33:325–347. [PubMed: 20367448]
60. Djouhri L, Newton R, Levinson SR, Berry CM, Carruthers B, Lawson SN. Sensory and electrophysiological properties of guinea-pig sensory neurones expressing Nav 1.7 (PN1) Na+ channel alpha subunit protein. J Physiol. 2003; 546:565–576. [PubMed: 12527742]
61. Yang Y, Wang Y, Li S, Xu Z, Li H, Ma L, Fan J, Bu D, Liu B, Fan Z, Wu G, Jin J, Ding B, Zhu X, Shen Y. Mutations in SCN9A, encoding a sodium channel alpha subunit, in patients with primary erythermalgia. J Med Genet. 2004; 41:171–174. [PubMed: 14985375]
62. Cummins TR, Dib-Hajj SD, Waxman SG. Electrophysiological properties of mutant Nav1.7 sodium channels in a painful inherited neuropathy. J Neurosci. 2004; 24:8232–8236. [PubMed: 15385606]
63. Dib-Hajj SD, Rush AM, Cummins TR, Hisama FM, Novella S, Tyrrell L, Marshall L, Waxman SG. Gain-of-function mutation in Nav1.7 in familial erythromelalgia induces bursting of sensory neurons. Brain. 2005; 128:1847–1854. [PubMed: 15958509]
64. Hoeijmakers JG, Faber CG, Lauria G, Merkies IS, Waxman SG. Small-fibre neuropathies--advances in diagnosis, pathophysiology and management. Nat Rev Neurol. 2012; 8:369–379. [PubMed: 22641108]
65. Faber CG, Hoeijmakers JG, Ahn HS, Cheng X, Han C, Choi JS, Estacion M, Lauria G, Vanhoutte EK, Gerrits MM, Dib-Hajj S, Drenth JP, Waxman SG, Merkies IS. Gain of function Nanu1.7 mutations in idiopathic small fiber neuropathy. Ann Neurol. 2012; 71:26–39. [PubMed: 21698661]
66. Ahmad S, Dahllund L, Eriksson AB, Hellgren D, Karlsson U, Lund PE, Meijer IA, Meury L, Mills T, Moody A, Morinville A, Morten J, O'Donnell D, Raynoschek C, Salter H, Rouleau GA, Krupp

JJ. A stop codon mutation in SCN9A causes lack of pain sensation. Hum Mol Genet. 2007; 16:2114–2121. [PubMed: 17597096]

67. Cox JJ, Reimann F, Nicholas AK, Thornton G, Roberts E, Springell K, Karbani G, Jafri H, Mannan J, Raashid Y, Al-Gazali L, Hamamy H, Valente EM, Gorman S, Williams R, McHale DP, Wood JN, Gribble FM, Woods CG. An SCN9A channelopathy causes congenital inability to experience pain. Nature. 2006; 444:894–898. [PubMed: 17167479]
68. Goldberg YP, MacFarlane J, MacDonald ML, Thompson J, Dube MP, Mattice M, Fraser R, Young C, Hossain S, Pape T, Payne B, Radomski C, Donaldson G, Ives E, Cox J, Younghusband HB, Green R, Duff A, Boltshauser E, Grinspan GA, Dimon JH, Sibley BG, Andria G, Toscano E, Kerdraon J, Bowsher D, Pimstone SN, Samuels ME, Sherrington R, Hayden MR. Loss-of-function mutations in the Nav1.7 gene underlie congenital indifference to pain in multiple human populations. Clin Genet. 2007; 71:311–319. [PubMed: 17470132]
69. Dib-Hajj SD, Yang Y, Black JA, Waxman SG. The Na(V)1.7 sodium channel: From molecule to man. Nat Rev Neurosci. 2013; 14:49–62. [PubMed: 23232607]
70. Hara T, Chiba T, Abe K, Makabe A, Ikeno S, Kawakami K, Utsunomiya I, Hama T, Taguchi K. Effect of paclitaxel on transient receptor potential vanilloid 1 in rat dorsal root ganglion. Pain. 2013; 154:882–889. [PubMed: 23602343]
71. Trimmer JS, Rhodes KJ. Localization of voltage-gated ion channels in mammalian brain. Annu Rev Physiol. 2004; 66:477–519. [PubMed: 14977411]
72. Black JA, Dib-Hajj S, McNabola K, Jeste S, Rizzo MA, Kocsis JD, Waxman SG. Spinal sensory neurons express multiple sodium channel alpha-subunit mRNAs. Brain Res Mol Brain Res. 1996; 43:117–131. [PubMed: 9037525]
73. Ho C, O'Leary ME. Single-cell analysis of sodium channel expression in dorsal root ganglion neurons. Mol Cell Neurosci. 2011; 46:159–166. [PubMed: 20816971]

Box Summary

What we already know about this topic

- Chemotherapy-induced peripheral neuropathy is a major clinical problem caused by agents such as paclitaxel.

What this article tells us that is new

- In rats the spontaneous activity of medium and large neurons was increased after paclitaxel treatment.
- Gene array studies demonstrated that the expression of several ion channels was altered by paclitaxel treatment potentially providing an explanation for the electrophysiological changes.

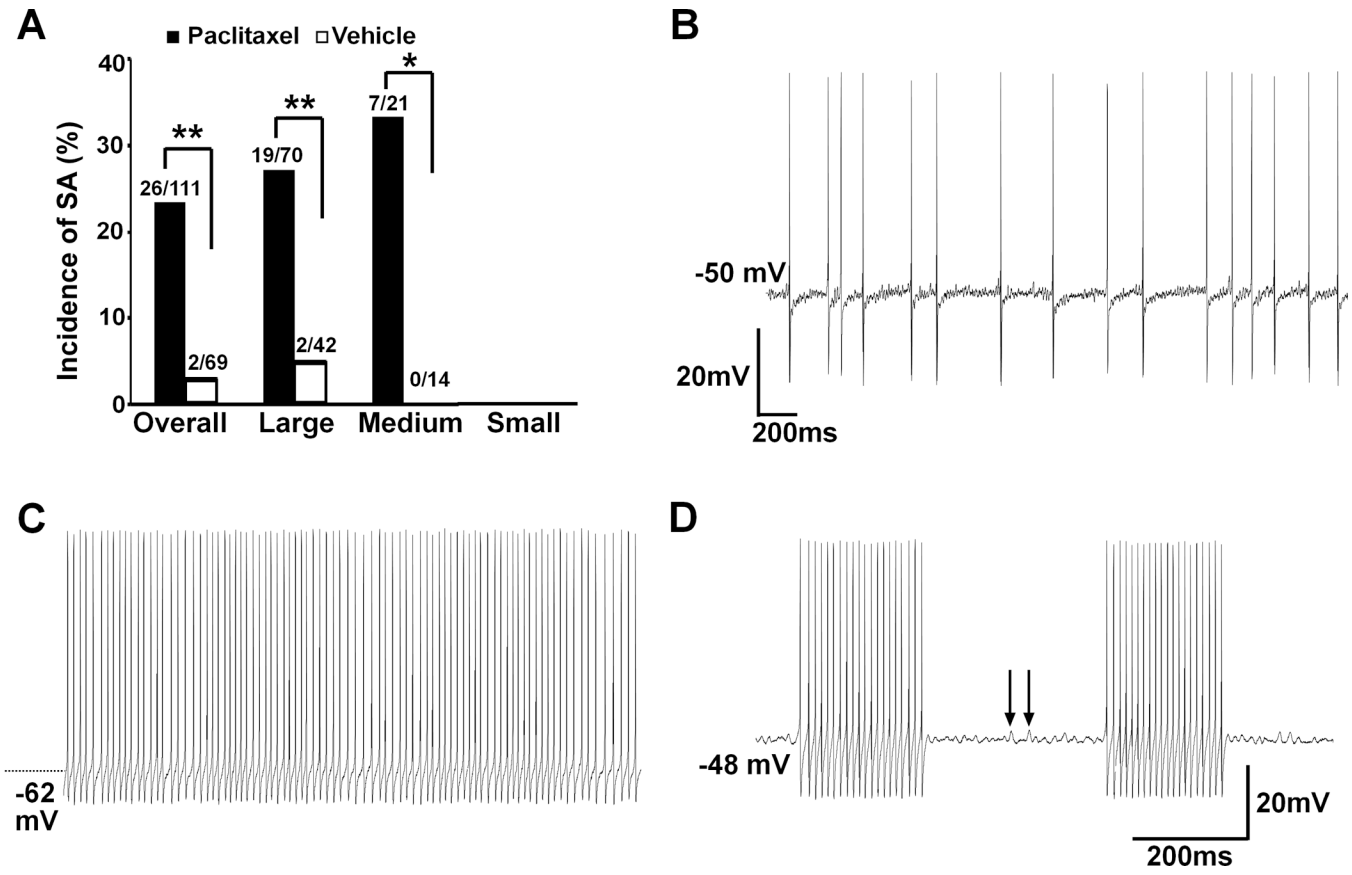

Fig. 1.

Increased incidence of spontaneous activity (SA) in dorsal root ganglion (DRG) neurons from animals with paclitaxel neuropathy. (A) Paclitaxel chemotherapy induced a significant increase of SA from DRG myelinated neurons including large ($P = 0.003$) and medium-sized ($P = 0.027$) neurons. * $P < 0.05$, ** $P < 0.01$, Chi-square test. (B) An example of irregular SA recorded from a medium-sized neuron, noticing the subthreshold membrane potential oscillations between each discharge. (C) Continuous discharges were recorded from a spontaneously active large neuron. (D) Spontaneous bursting discharges were recorded from a large neuron after paclitaxel chemotherapy. Subthreshold oscillations (arrows) were obvious between each episode of bursting discharges (arrow).

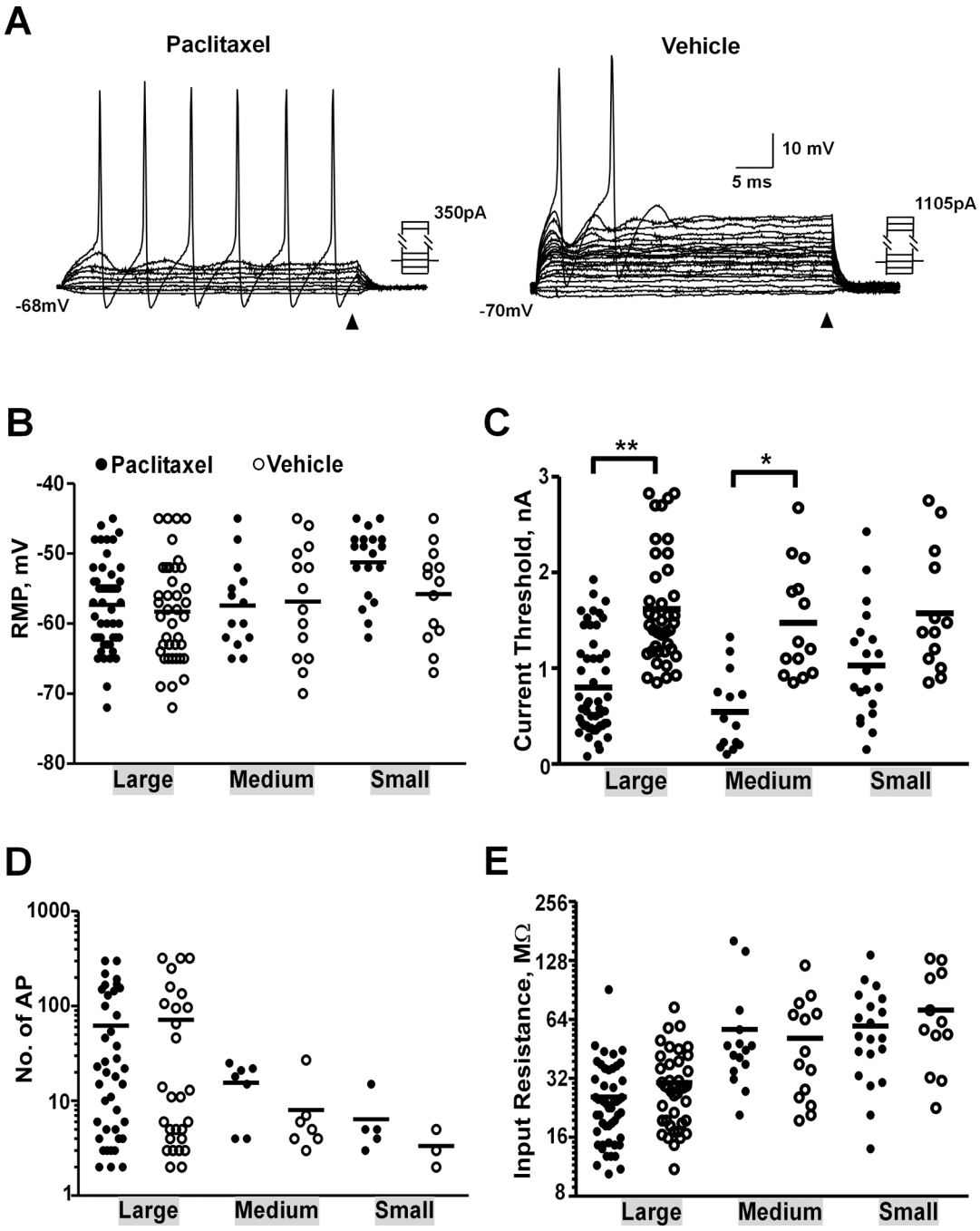

Fig. 2.

Dorsal root ganglion (DRG) neurons showed increased excitability after paclitaxel chemotherapy. (A) Sample recordings of large neurons from paclitaxel- and vehicle-treated animals. The input resistance of each cell was measured based on the steady-state voltage changes at the end of the application of a series of hyperpolarizing/depolarizing currents as indicated by arrowhead. Comparison of electrophysiological properties of DRG neurons with different size, including resting membrane potential (RMP) (B), current threshold (C), number of action potentials (AP) induced by a 1-sec 2 X current threshold intracellular

depolarizing current (D) and input resistance (E). * $P < 0.001$, ** $P < 0.0001$, One-way ANOVA.

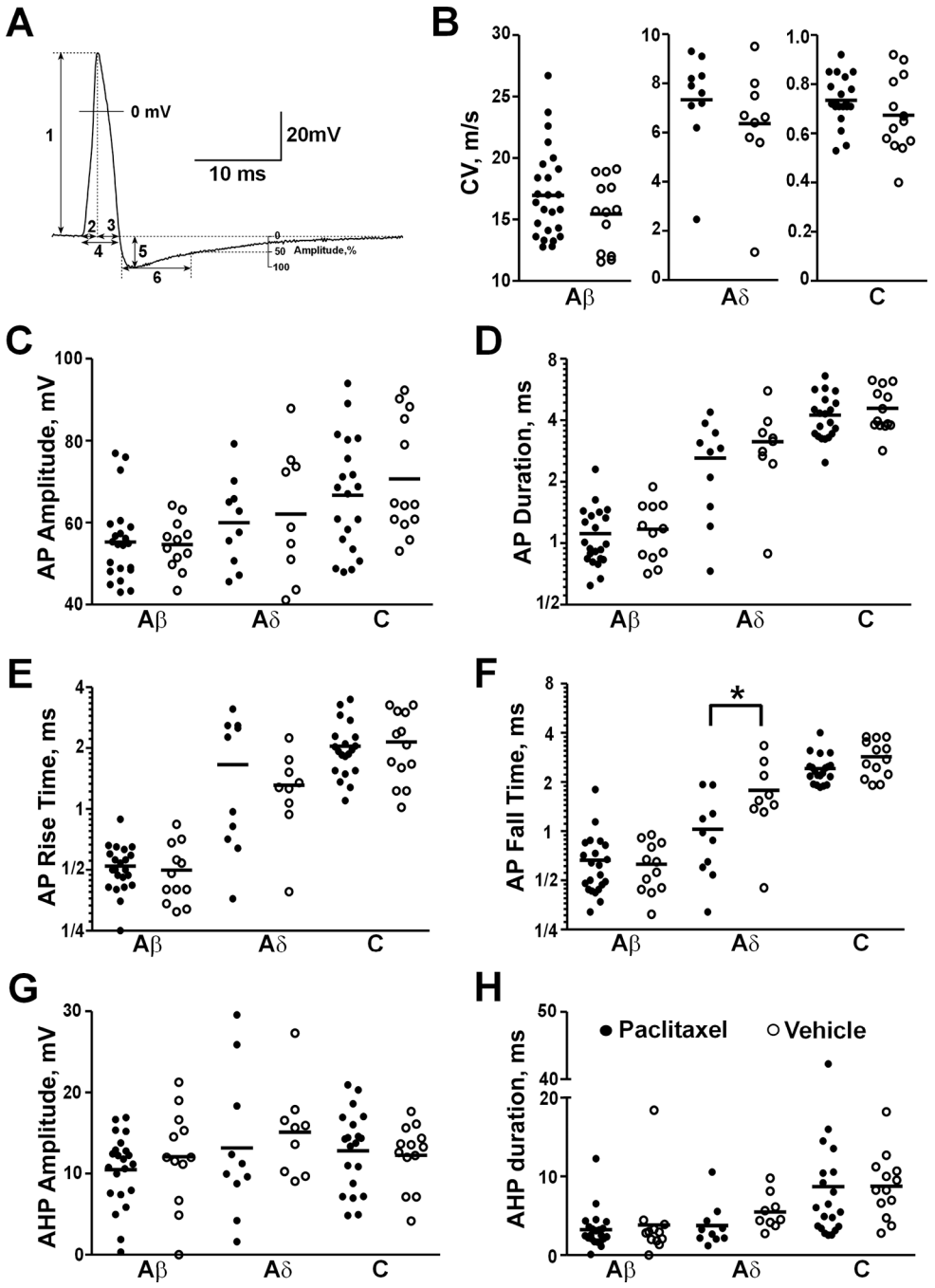

Fig. 3.

Dorsal root ganglion (DRG) neurons showed similar conduction velocity (CV) and action potential (AP) properties after paclitaxel chemotherapy. (A) AP was recorded intracellularly from soma of a C-neuron evoked by peripheral nerve stimulation. AP properties were measured as illustrated: (1) AP amplitude, (2) AP rise time, (3) AP fall time, (4) AP duration at base, (5) afterhyperpolarization (AHP) amplitude, (6) AHP 50% duration. Comparisons of CV (B), AP amplitude (C), AP duration (D), AP rise time (E), AP fall time (F), AHP

amplitude (G) and AHP 50% duration (H) were made after paclitaxel chemotherapy. * P < 0.05, One-way ANOVA.